

Drosophila melanogaster Scramblases modulate synaptic transmission

Usha Acharya,^{1,2} Michael Beth Edwards,¹ Ramon A. Jorquera,^{3,5} Hugo Silva,³ Kunio Nagashima,⁴ Pedro Labarca,³ and Jairaj K. Acharya¹

¹Laboratory of Protein Dynamics and Signaling, National Cancer Institute Frederick, Frederick, MD 21702

²Program in Gene Function and Expression, University of Massachusetts Medical School, Worcester, MA 01605

³Centro de Estudios Científicos, Valdivia 511-0246, Chile

⁴EM Facility/Image Analysis Laboratory, Science Applications International Corporation Frederick, Frederick, MD 21702

⁵Universidad Austral de Chile, Valdivia 509-9200, Chile

Scramblases are a family of single-pass plasma membrane proteins, identified by their purported ability to scramble phospholipids across the two layers of plasma membrane isolated from platelets and red blood cells. However, their true *in vivo* role has yet to be elucidated. We report the generation and isolation of null mutants of two Scramblases identified in *Drosophila melanogaster*. We demonstrate that flies lacking either or both of these Scramblases are not compromised *in vivo* in processes requiring scrambling of phospholipids.

Instead, we show that *D. melanogaster* lacking both Scramblases have more vesicles and display enhanced recruitment from a reserve pool of vesicles and increased neurotransmitter secretion at the larval neuromuscular synapses. These defects are corrected by the introduction of a genomic copy of the *Scramb 1* gene. The lack of phenotypes related to failure of scrambling and the neurophysiological analysis lead us to propose that Scramblases play a modulatory role in the process of neurotransmission.

Introduction

Scramblases are a family of four proteins in humans and mice. They are conserved across species, and at least one member of this family is encoded in organisms ranging from yeast to human beings (Sims and Wiedmer, 2001). Human Scramblase 1 (PLSCR1) was initially identified as a protein thought to be involved in facilitation of transbilayer movement of phospholipids across the plasma membrane (Basse et al., 1996; Comfurius et al., 1996; Zhou et al., 1997). Many cell membranes harbor a Ca^{2+} -dependent mechanism that can facilitate transbilayer movement of phospholipids between the two leaflets, leading to loss of membrane lipid asymmetry termed scrambling. Scrambling is observed in platelets, erythrocytes, and other cells after elevated intracellular Ca^{2+} and cell injury by complement and also in cells undergoing phagocytosis and apoptosis (Zwaal et al., 2005). Attempts to purify and clone proteins active in scrambling led to the identification of human

PLSCR1. Scramblases are type 2 single-pass transmembrane proteins (Zhou et al., 1997). The four members identified in mice and humans have been named PLSCR1 through -4. All except PLSCR2 contain a proline-rich NH_2 -terminal domain with PXXP and PPXX motifs that can potentially bind to SH3 and WD40 domain-containing proteins. An intracellular EF hand, a Ca^{2+} binding motif, precedes the transmembrane segment. Mice lacking two of these Scramblases, 1 and 3, were recently generated. Cells derived from PLSCR1-null mice showed alterations in granulocyte production in response to growth factors and antiviral response to interferon (Zhou et al., 2002). PLSCR3-null mice and double mutants of PLSCR1 and -3 nulls showed adiposity, dyslipidemia, and insulin resistance (Wiedmer et al., 2004). Neither of the knockout mice shows defects in events associated with lipid scrambling. This suggests either that the other two members of the PLSCR family maintain Scramblase activity or that the presumed activity of this protein in scrambling is incorrect. Hence, the actual *in vivo* biological function of members of the Scramblase family has yet to be elucidated.

The *Drosophila melanogaster* genome encodes two ubiquitously expressed proteins with strong sequence homology to mice and human Scramblases. Using a reverse genetic approach, we have generated flies lacking each of the two Scramblases

M.B. Edwards, R. Jorquera, and H. Silva contributed equally to this paper.

Correspondence to Jairaj K. Acharya: acharyaj@mail.ncifcrf.gov

Abbreviations used in this paper: dsRNA, double-stranded RNA; ECP, exo/endo pool of SVs; EMS, ethyl methane sulfonate; GMR, glass multimer reporter; NMJ, neuromuscular junction; PS, phosphatidylserine; PTP, posttetanic potentiation; RP, reserve pool; S2 cells, Schneider cells; SV, synaptic vesicle; UAS, upstream activating sequence.

The online version of this article contains supplemental material.

individually and flies lacking both Scramblases. Our studies using these mutants indicate that Scramblases do not play a deterministic role in scrambling of phospholipids that accompanies developmentally regulated apoptosis or in immune responses involving phagocytosis of bacterially infected cells. Further analyses indicate that Scramblases play a modulatory role in the process of neurotransmission at the larval neuromuscular junction (NMJ).

Results

D. melanogaster Scramblases

The deduced sequences of the mammalian PLSCR family of proteins reveal them to be type 2 plasma membrane proteins with the transmembrane domain at the COOH terminus and a proline- and cysteine-rich acidic domain. The NH₂-terminal segments contain PXXP and PPXY sequences that are potential SH3 and WW domain binding sites, respectively. The COOH-terminal ends of the proteins are conserved and contain a putative Ca²⁺ binding motif proximal to the transmembrane domain. There is considerable sequence variation at the NH₂-terminal segment of Scramblases. The PLSCR2 member of the family lacks the NH₂-terminal proline- and cysteine-rich sequence. *D. melanogaster* genome analysis identifies two genes with significant homology to mammalian Scramblases (Fig. 1 A; Drysdale et al., 2005). These are CG32056 and CG1893. Protein encoded by CG32056 Scramb 1 shows 37% identity with mouse Scramb 1 (PLSCR1) protein, whereas that of CG1893 or Scramb 2 protein shows 41% identity with Scramb 2 (PLSCR2). The Scramb 1 and 2 proteins of *D. melanogaster* are 56% identical and 69% similar to each other (Fig. 1 A). Although Scramb 1 includes the proline-rich region NH₂-terminal domains with PXXP and PPXY motifs that bind SH3 and WD40 region, Scramb 2 protein lacks this stretch of amino acids and in this regard is closer to mammalian Scramb 2 protein. A third gene, CG9804, has been labeled as Scramblase in the annotated genome. However, this protein shows only 25% identity with either mammalian or

the *D. melanogaster* Scramblases and seems to have branched out earlier during evolution. Moreover, unlike the other two *D. melanogaster* proteins, this protein has restricted expression, as we fail to see ubiquitous expression by Western analysis (unpublished data). CG10427 stated as a Scramblase in the Flybase was annotated as an uncertain gene and has been eliminated in release 3 of the genome annotation (this aberration resulted from annotation errors of CG32056 gene region).

To profile the tissue and developmental expression of Scramblases in *D. melanogaster*, we have generated polyclonal antibodies against both Scramb 1 and 2 proteins and in addition have obtained monoclonal antibodies against Scramb 1 protein. We have also succeeded in expressing a GFP-tagged version of Scramb 2 using the upstream activating sequence (UAS)-Gal4 system (Brand and Perrimon, 1993). Western blot analysis of wild-type *D. melanogaster* demonstrates that the two proteins are expressed ubiquitously and throughout development (Fig. 1 B). Lower levels are observed by Western analysis in early embryos before cellularization. The low abundance in early embryos is attributable to the fact that these are predominantly plasma membrane proteins (see below and Fig. S1, available at <http://www.jcb.org/cgi/content/full/jcb.200506159/DC1>). The *D. melanogaster* embryo begins as a single cell and a syncitium before undergoing cellularization, and the plasma membrane surface grows ~30-fold during cellularization of the syncytial embryo. Immunofluorescence localization and analysis of transgenic flies (GFP-Scramb 2 fusion) localize the proteins predominantly to the plasma membrane (not depicted). We have colocalized Scramb 1 protein with HRP antigen at the plasma membrane in the larval neurons and the Scramb 2 protein with Notch that localizes to the plasma membrane at the apical margins of the cells of the larval eye-antennal anlagen (Fig. S1). Although Scramb 2 is homogeneously localized at the plasma membrane, Scramb 1 shows a nonhomogenous distribution along the plasma membrane, with areas of intense staining interspersed with areas of homogenously strong staining. The localization of the two proteins suggests a role for them in



Figure 1. Scramblases are evolutionarily conserved and ubiquitously expressed. (A) Comparison of the amino acid sequences of *Saccharomyces cerevisiae* Scramblase homologue, *YJR100cp*, *D. melanogaster* Scramb 1 and 2 (DmScramb 1 and 2), and human Scramblases 1–4 (HsPLSCR1–4) proteins using multiple sequence alignment and box shade programs. (B) Extracts were prepared from *D. melanogaster* during various stages of development as indicated, and 5 µg of extracts were loaded on gel and probed for Scramb 1 and 2 protein as indicated. Blots were reprobed for tubulin as loading controls.

events involving the plasma membrane. Because the in vivo role of Scramblases in lipid scrambling and other cellular functions remains unresolved, we decided to generate mutant flies lacking the family of Scramblases and then carry out functional analyses.

Generation and isolation of Scramblase mutants

We have used a Western blot-based reverse genetics approach to obtain mutants for both Scramblase genes in *D. melanogaster* (Dolph et al., 1993; Acharya et al., 1998). The lack of predictable phenotypes defining the mutant complicates many genetic screens. Therefore, we used a previously documented Western blot-based screening strategy that monitors loss of protein expression (loss of Scramblase expression in our case) on immunoblots (Dolph et al., 1993; Acharya et al., 1998). In this protocol, male flies are randomly mutagenized, by feeding them the chemical mutagen, ethyl methane sulfonate (EMS). Mutagenized males are crossed to female balancer flies. Balanced progeny are crossed to flies with a large chromosomal deficiency that uncovers the genomic interval including the *Scramb 1* gene. Single heads from flies trans-heterozygous for the deficiency and a mutagenized third chromosome are screened for the loss of Scramb 1 antigen by Western blots (Fig. 2 A). From a screen of 1,950 EMS-mutagenized third chromosomes, 1,900 lines that were viable in trans to *Df(3L)AC1, r^{nroe-1}p^p* were obtained. Western analysis of these lines identified a mutant line expressing no Scramb 1 protein (Fig. 2 A, bottom). The *Scramb 1* gene was isolated from this mutant and subjected to sequence analysis. The *scramb1*-null mutant had a T-to-A transition in the first intron of the coding region. This leads to a splicing defect (confirmed by RT-PCR across intron 1) and truncation of the protein after 38 amino acids (+ 3 amino acids of the intron).

Thus, the *scramb1* mutant is either a null allele or a severely hypomorphic mutant.

Likewise, in the *Scramb 2* screen, 2,100 lines, viable in trans over *Df(3L)M21(kni[ri-1]p)* were established and screened by Western analysis (Fig. 2 B, top). One of the lines showed no antigen reactivity against the Scramb 2 antibody (Fig. 2 B, bottom). Sequencing of the *Scramb 2* gene from this line showed a T-to-A transition at the first exon–intron junction. In this instance, the splicing defect (confirmed by RT-PCR) leads to termination of the gene after 57 amino acids (an additional eight amino acids from read-through in the intron). Hence, the *scramb2* mutant is either a null or severely hypomorphic mutant. Both mutants were backcrossed three times to *w1118* (control) to outcross all background mutations.

The two mutants are null (or severely hypomorphic) for the respective normal Scramblase proteins. Double mutants of *scramb1* and -2 were generated by meiotic recombination of the individual mutants. The double mutants do not express both proteins as confirmed by Western analysis and also by immunofluorescence at the larval NMJ (Fig. 2 and Fig. S2, available at <http://www.jcb.org/cgi/content/full/jcb.200506159/DC1>). Because the in vivo role of Scramblases in lipid scrambling has not been unequivocally established, we analyzed the mutants in events requiring scrambling of phospholipids, including the exposure of phosphatidylserine (PS) on cell surface in cells undergoing apoptosis and phagocytosis.

Scramblase mutants show no defects in developmentally regulated and ectopically induced apoptotic events in vivo
scramb1, *scramb2*, and the double mutants are homozygous viable. Programmed cell death is an important feature of *D. melanogaster* development and tissue homeostasis.

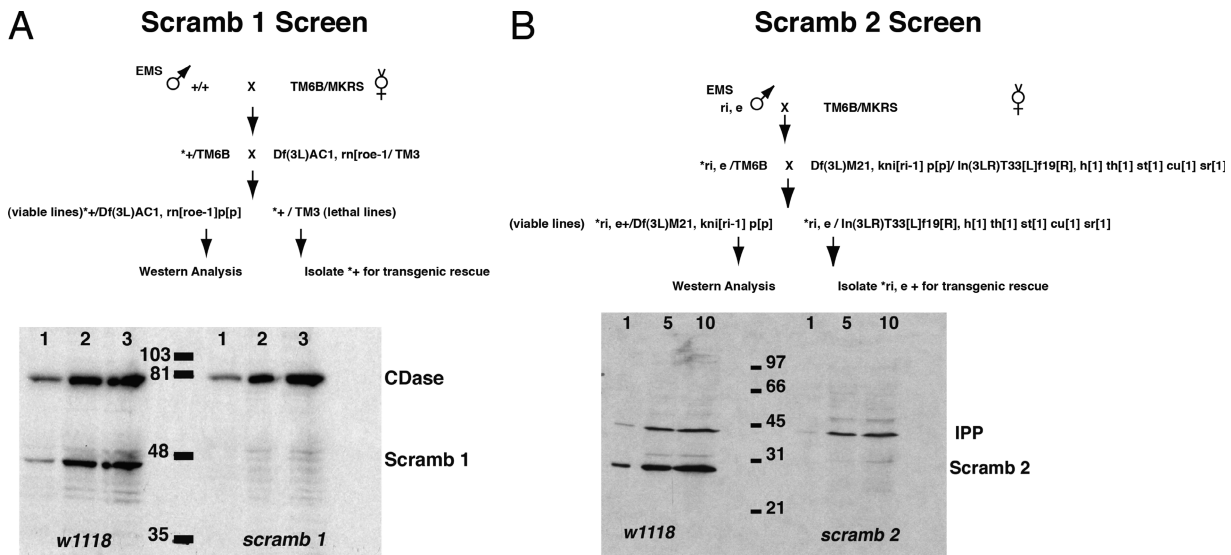


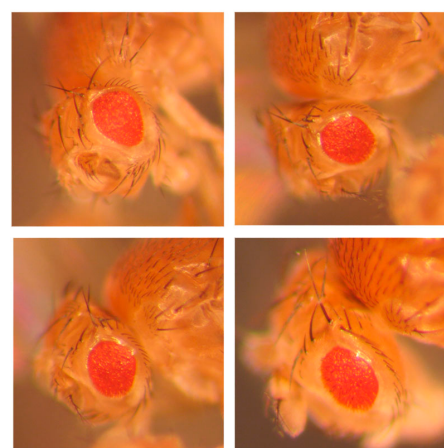
Figure 2. Generation and isolation of Scramblase mutants. (A) The genetic scheme to isolate the *scramb1* mutant. (B) The scheme to obtain mutants in Scramb 2. The Western blot analysis of the null mutants is shown below the schemes. For *scramb1*, analysis of 1, 2, and 3 head extracts were loaded and probed. The blot was probed for *D. melanogaster* ceramidase (CDase) as loading control (Acharya et al., 2003, 2004). In the blot for *scramb2*-null mutant analysis, 1, 5, and 10 head worth of extracts from control *w1118* and the mutant were loaded and probed for the protein. The blots were probed for Inositol polyphosphate 1-phosphatase (IPP) as loading control (Acharya et al., 1998).

During development, excess cells and tissues that are no longer useful are removed by apoptosis, and mutants that fail to undergo such normal apoptosis do not survive past embryogenesis (White et al., 1994). Because Scramblase mutants are viable and fertile and show no developmental defects, apoptosis during development is clearly not compromised in these mutant flies. As in mammals, apoptotic cell death in *D. melanogaster* is also characterized by PS exposure and clearance of cells by phagocytosis (van den Eijnde et al., 1998). In *D. melanogaster*, reaper, hid, and grim genes are necessary for induction of apoptosis. Ectopic overexpression of any of these genes in the fly eye using the eye-specific driver GMR (glass multimer reporter) causes normal photoreceptors to undergo apoptotic cell death, resulting in a severe eye ablation phenotype (Nordstrom et al., 1996). To determine whether Scramblase mutants can modulate this phenotype, we examined eyes from flies overexpressing reaper in each of the three mutant backgrounds. The eye sizes were not significantly different in the three mutant backgrounds compared with control flies (Fig. 3). This indicates that the dynamics of reaper-mediated apoptotic cell death is not altered in Scramblase mutant backgrounds. Because the eye sizes were not different between the control *w1118* and mutant flies, PS-mediated cell death and phagocytic clearance of apoptotic cells were clearly unaffected in the mutant backgrounds. Thus, Scramblases are not required for either programmed or ectopically triggered apoptotic cell death.

Scramblase mutants can mount an effective response to infection with microorganisms

Immune defense mechanisms in *D. melanogaster*, like in other metazoan organisms, include physical barriers to infection, innate, and humoral responses (Lavine and Strand, 2002; Hoffmann, 2003; Brennan and Anderson, 2004; Leclerc and Reichhart, 2004). The immune hemocyte cells, for example, mediate cellular responses such as phagocytosis, encapsulation, and melanization, as well as produce humoral effector proteins. Phagocytic cells recognize a variety of signals on cells primed for phagocytosis (such as apoptotic and bacterially infected cells), including cell surface exposure of PS. We decided to evaluate whether the absence of Scramblases compromised any of these functions, resulting in an observable phenotype. We therefore infected wild-type and mutant cells with a mixture of gram positive and negative microorganisms as described in Materials and methods (Rodriguez et al., 1996; Bernal and Kimbrell, 2000). Immune competence is measured as viability of flies over

CyO 2X Gmr-rpr ; + CyO 2X Gmr-rpr ; scramb1



CyO 2X Gmr-rpr ; scramb2 CyO 2X Gmr-rpr ; scramb1, scramb2

Figure 3. Scramblase mutants can undergo apoptotic cell death and mount an effective immune response. Two copies of reaper were expressed under the control of GMR promoter. Expression of reaper results in apoptotic cell death of photoreceptors. Expression in *scramb1*, *scramb2*, or the double mutant did not affect reaper-induced apoptosis.

time, as shown in Table I. The resistance to an inoculum of mixed microorganisms was comparable between the control *w1118* and mutant backgrounds. Thus, the immune competence of Scramblase mutants is similar to wild-type flies and not compromised.

We conclude that Scramblases do not play a critical role in in vivo events that involve scrambling of phospholipids, such as exposure of PS to the outer leaflet and immunoreactive mechanisms for phagocytic clearance of bacterially infected cells. To demonstrate that PS exposure, a process requiring scrambling of phospholipids, was not compromised in backgrounds where Scramblase protein levels are perturbed, we conducted a series of experiments using *D. melanogaster* Schneider (S2) cells in which we either overexpressed the two Scramblases or depleted them using RNAi.

Increased expression or knock down of Scramblases in S2 cells does not affect PS exposure on cell surface

Exposure of cell surface PS during apoptosis has been used as a measure of the ability of cells to scramble phospholipids (Schlegel et al., 2000; Tepper et al., 2000; Wolfs et al., 2005). An early event in apoptosis is exposure of PS on the cell surface, which can be analyzed by binding of fluorescently labeled annexin V

Table I. Survival after infection with mixed microorganisms

Days after infection	Percentage of flies surviving (\pm SD)			
	<i>w1118</i>	<i>scramb1</i>	<i>scramb2</i>	Double mutant
1	88 \pm 5.6	82 \pm 5.5	82 \pm 8.1	82 \pm 3.2
2	69 \pm 7.1	67 \pm 7.2	62 \pm 4.9	63 \pm 7.0
3	52 \pm 2.1	55 \pm 1.5	50 \pm 7.6	50 \pm 4.2
4	43 \pm 3.6	46 \pm 4.2	46 \pm 5.6	45 \pm 4.0

3-dold control *w1118*, *scramb1*, *scramb2*, and the double-mutant flies were individually infected with a mixed microorganism culture, as described in Materials and methods. After the flies recovered from the effects of anesthesia, they were set up in vials in groups of 10 and observed over the next 2 wk, and percentage of survival was calculated. Because the mortality was not affected 4 d after infection in all the samples studied, only data for 4 d after infection has been included.

that has a high affinity for cell surface PS. The impermeant nucleic acid dye propidium iodide is used in conjunction to exclude cells whose plasma membrane integrity is compromised (necrotic or damaged). To visualize the process of scrambling (i.e., exposure of PS in cells with altered Scramblase expression), we used *D. melanogaster* S2 cells to knock down or over-express Scramblase and follow PS exposure. Scramb 1 and 2 proteins were knocked down separately or together by RNAi treatment in S2 cells by transfecting with double-stranded RNA (dsRNA) as described in Materials and methods. Western blot analysis of dsRNA-treated cell lysates (+) shows significant depletion of Scramb 1 and 2 compared with untreated lysates (Fig. 4, A and B). S2 cells after dsRNA treatment were incubated in a Ca^{2+} -rich medium containing fluorescently labeled annexin V and propidium iodide. PS exposure was measured as percentage of cells that stained positive for annexin V but negative for propidium iodide (Fig. 4 D, % scrambling). As seen in Fig. 4 D (–Act D), there is no difference between control S2 cells and Scramb 1, Scramb 2, and the double (Scramb 1, Scramb 2) knockdown cells. We then tested whether scrambling would be compromised in Scramblase knockdown cells undergoing apoptosis. It has previously been shown that *D. melanogaster* S2 cells undergo apoptosis and expose PS when treated with Actinomycin D (Zimmermann et al., 2002). Using similar conditions, apoptosis was induced in S2 cells by Actinomycin D treatment, and PS exposure was measured as before. There were no apparent differences in the ability of these cells to expose their cell surface PS (Fig. 4 D, +Act D) as compared with non-RNAi-treated cells undergoing apoptosis.

We then stably overexpressed Scramb 1 and 2 proteins under the control of the metallothionein promoter (Bunch et al., 1988). Fig. 4 C depicts Western blots showing dramatic inducible

expression of both Scramblases. PS exposure was measured in these cells overexpressing Scramblases. There was no significant difference in the number of cells that were annexin V positive and propidium iodide negative between the control and over-expressors (Fig. 4 E, % scrambling). The baseline apoptosis was itself slightly higher, probably because of the addition of 0.5 mM copper sulfate to induce protein expression (Fig. 4 E, –Act D). Next, we induced apoptosis in S2 cells overexpressing Scramb 1 or 2 protein by Actinomycin D treatment and evaluated PS exposure by annexin V binding assays. There was no difference between the vector-transfected control and the overexpressing stable cells (Fig. 4 E, +Act D). Thus, neither knock down or overexpression of Scramblases resulted in altered exposure of PS in resting cells as well as in cells undergoing apoptosis.

The results described above lead us to believe that Scramblases do not play a determining role in scrambling of phospholipids in *D. melanogaster*. We then sought to evaluate the actual in vivo functions of this family of proteins. The Scramblase double-mutant flies appear visibly more active in a vial compared with either of the single mutants or the control *w1118* flies. Hyperactivity has been associated with neurological alterations in *D. melanogaster* (Wang et al., 1997; Ghezzi et al., 2004). Because the double mutants were hyperactive and because Scramblases are ubiquitously expressed in the plasma membrane, the *D. melanogaster* NMJ was analyzed in our mutant for defects in synaptic structure and function. *D. melanogaster* larval NMJ is extremely active with intracellular and intercellular signaling involving a plethora of signal-transduction cascades active across plasma membranes at the junction (Keshishian et al., 1996; Rodesch and Broadie, 2000; Keshishian, 2002; Kidokoro et al., 2004; Kuromi and Kidokoro, 2005). We rationalized that the structure and function would be sensitive to loss

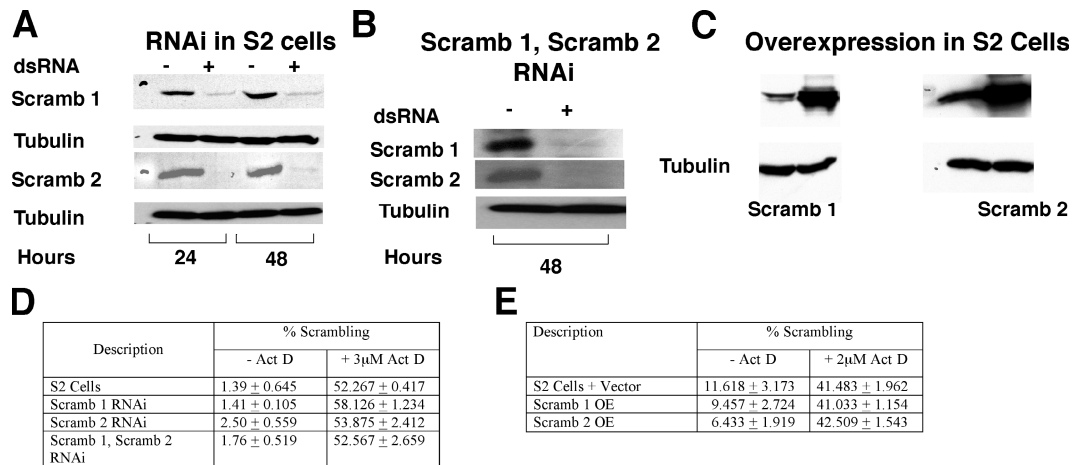


Figure 4. Scramblase proteins are not involved in cell surface exposure of PS. (A) S2 cells were transfected with Scramb 1 or 2 dsRNA, and cells were harvested 24 and 48 h after transfection and analyzed by Western analysis for Scramb 1 or 2 protein. Both Scramb 1 and 2 are down-regulated tremendously by RNAi-mediated knockdown. The extracts were probed for tubulin as loading controls. (B) Both Scramb 1 and 2 were knocked down in S2 cells simultaneously, and cells were assayed for protein 48 h after transfection. Both proteins are down-regulated in this experiment. (C) Stable cell lines overexpressing Scramb 1 or 2 proteins under the control of a metallothionein promoter were established. Both proteins are massively expressed upon induction in these cells. The extracts were probed for tubulin as controls. (D) The percentage of cells that stain positively for annexin V binding and negatively for propidium iodide were counted and plotted as percentage of scrambling. (D) Annexin V-positive cells in those that have undergone RNAi-mediated knockdown. (E) Scramblase overexpressing cells. RNAi-mediated knockdown cells were subject to 3 μ M Actinomycin D for 3 h, and the percentage of scrambling cells was determined (D; +Act D column). As the baseline percentage of apoptotic cells was slightly higher in cells overexpressing Scramblase (E; –Act D column; probably due to the addition of 1 mM copper sulfate to induce protein), 2 μ M Actinomycin D was used and the percentage of scrambling calculated (E; +Act D column).

of Scramblase proteins if they had an important role in events involving the plasma membrane.

Scramblase mutants show altered synaptic function and increased release of neurotransmitters

We verified the expression of Scramb 1 and 2 at the larval NMJs by immunofluorescence colocalization with synaptotagmin and HRP (Fig. 5). We also performed coimmunolocalization of Scramb 2 with disc large, cysteine string protein, syntaxin, and Fasciclin II (Fig. S4, available at <http://www.jcb.org/cgi/content/full/jcb.200506159/DC1>). Scramb 1 and 2 proteins are expressed in all segmental nerves and presynaptic and postsynaptic membranes of the larval NMJs (Figs. 5, S3, and S4). We then undertook ultrastructural examination and analysis of the active zones (Babcock et al., 2004; Rohrbough et al., 2004). The analysis revealed a significant increase in the number of synaptic vesicles (SVs) and more vesicles docked at the active one (Fig. 6 and Table II). The single mutants, on the other hand, did not show significant changes in the ultrastructure of NMJs, except that there was more than one docked vesicle at the active zone of most of the type 1b boutons examined (unpublished data).

We reasoned that an increased SV content in double-mutant synapse shown in EM studies should result in an increased loading of FM1-43 at nerve endings after massive vesicle mobilization. FM1-43 binds to membranes and remains trapped in SVs that undergo endocytosis. We analyzed the extent of FM1-43

loading in vesicles cycling through an exo/endo pool of SVs (ECP). Loading of ECP with FM1-43 was achieved by exposing boutons (5 min) to an external solution high in K⁺ in the presence of dye (Fig. 7 A; Delgado et al., 2000). Fluorescence brightness was analyzed 5 min after extensive perfusion with dye-free standard solution. Data analysis revealed that fluorescence brightness in double-mutant boutons was significantly above control (Fig. 7 A). After ECP loading, we subjected synapses to high-frequency stimulation of the nerve at 10 Hz in a standard external solution containing FM1-43, to also load vesicles cycling through a reserve pool (RP) of SVs. As shown in Fig. 7 B, this maneuver increases dye load, and fluorescence now distributes over the whole volume of synaptic boutons. Under these conditions also, fluorescence brightness in the double mutant was significantly above control (Fig. 7 B). Finally, to evaluate the extent of dye loading in SVs cycling through RP, synapses were exposed for a second round to a high K⁺ solution void of dye (3 min) to induce massive release of SVs in ECP. The fluorescence that remains after this second exposure to high K⁺ labels vesicles that are cycling through the RP (Delgado et al., 2000). Data analysis revealed that fluorescence brightness was significantly larger in double-mutant boutons (Fig. 7 C). Thus, our FM1-43-loading studies are consistent with EM data indicating an excess content of SVs in double-mutant presynaptic terminals. Importantly, as documented in Fig. 7, in all conditions, the extent of FM1-43 loading in the double mutant was rescued to control values by the introduction of a copy of the *Scramb 1* gene.

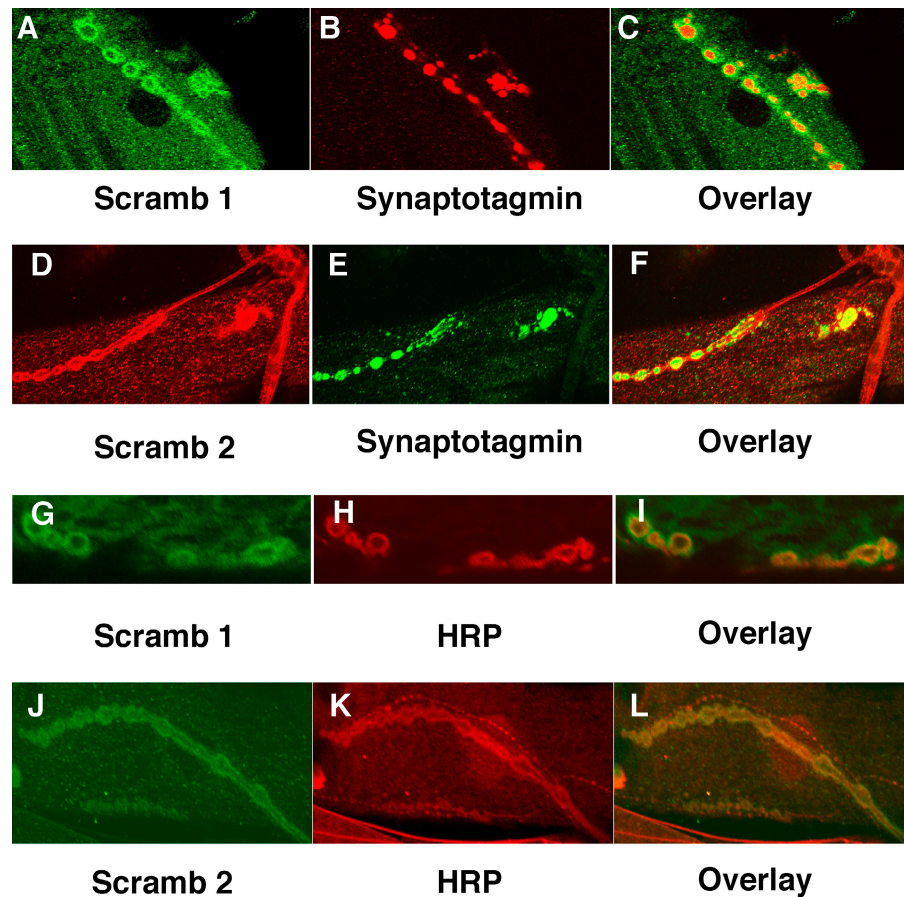


Figure 5. Scramblase proteins localize to the larval NMJs. The Scramblase proteins were localized by anti-Scramb 1 monoclonal (A and G) and rabbit anti-Scramb 2 polyclonal antibodies. Rabbit anti-synaptotagmin (B) or monoclonal (E) and anti-HRP (H and K) were used in coimmunolocalization. The overlays are shown in C, F, I, and L.

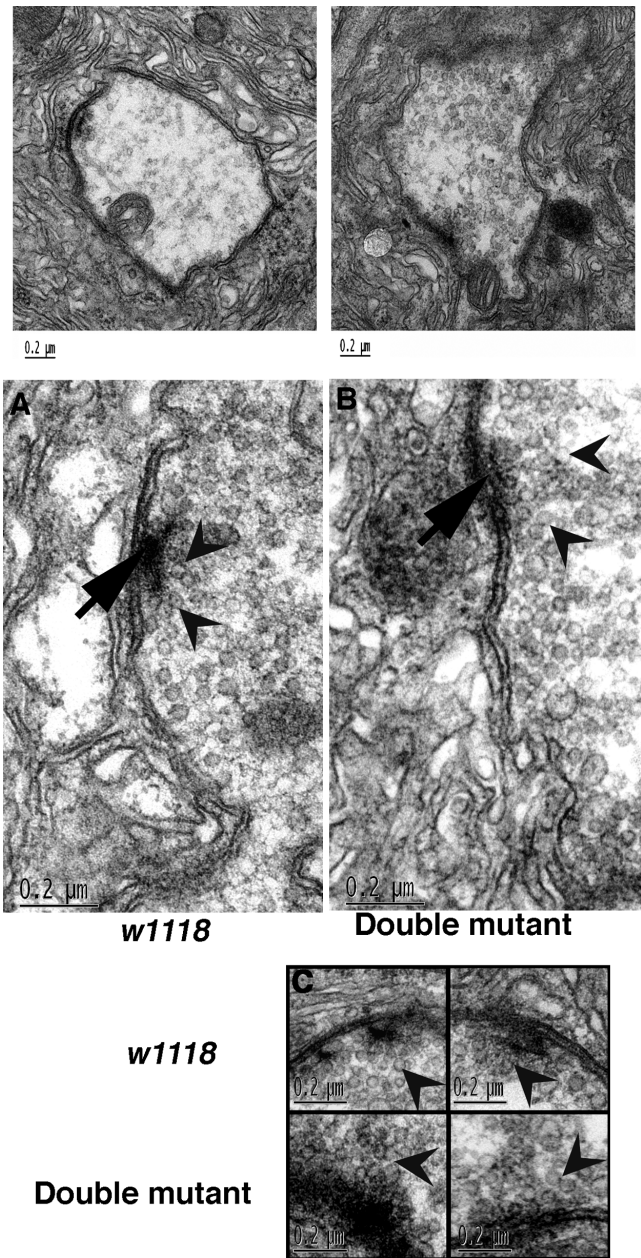


Figure 6. Scramblase mutants have an increased number of SVs in the active zone. (top) Transmission electron micrograph of a synaptic bouton from control *w1118* and the double mutant. (middle) Transmission EM comparison of the active zones from a control *w1118* and the double mutant. The arrows indicate the T-bar in the active zone. Arrowheads show the vesicles clustered close to this area. (bottom) The top two figures show the active zones from *w1118* type 1b synaptic boutons, and the bottom two figures are from the double mutants.

We then proceeded to investigate ECP exocytosis rate by monitoring the decay of FM1-4 fluorescence brightness after dye loading of vesicles through ECP during low-frequency stimulation of the nerve at 0.5 Hz. Under this condition, transmitter release is maintained essentially by mobilization of ECP (Kuromi and Kidokoro, 2000). We found that the time course of decline of fluorescence brightness was similar in double-mutant and control boutons, indicating similar properties of ECP exocytosis (unpublished data). We also investigated the recruitment

Table II. Comparison of SV distribution in the boutons, including around the active zones of control and double-mutant NMJs

Description	<i>w1118</i>	Double mutant
Number of vesicles	37.7 ± 1.1	60.7 ± 3.3
Cross-section (μM)	1.3 ± 0.1	1.2 ± 0.1
Clustered ($<0.25 \mu\text{M}$)	10.7 ± 1.1	25.2 ± 1.7
Docked	1.3 ± 0.3	4.1 ± 0.5
Nonclustered	27.0 ± 1.6	34.8 ± 2

of SVs from an RP. The RP contains a majority of SVs and has been implicated in use-dependent increase in transmitter release and is mobilized during high-frequency activity at the synapse (Delgado et al., 2000; Kuromi and Kidokoro, 2000). 5 min after dye loading of SVs cycling through the RP, RP recruitment rates were assessed by monitoring the decline in fluorescence brightness during high-frequency stimulation at 10 Hz. We found that the rate of RP recruitment was markedly enhanced in double-mutant boutons, as indicated by a significantly faster rate of fluorescence brightness decline ($2.4 \pm 0.2 \text{ min } [n = 10]$ vs. $8.5 \pm 0.3 \text{ min } [n = 10]$; Fig. 7 D). This result prompted us to investigate whether RP recruitment at rest, in the absence of high-frequency stimulation of the nerve, was also enhanced in the double mutant. Therefore, we evaluated the extent of fluorescence brightness decline at rest, 5 min after SVs cycling through RP were loaded with dye. As shown in Fig. 7 E (top) at rest, the decline in fluorescence brightness was markedly enhanced in double-mutant boutons (fivefold). Moreover, the extent of fluorescence decline induced by a 5-min stimulation of the nerve at 0.5 Hz in the double mutant was also significantly enhanced relative to control (Fig. 7 E, bottom). These results reveal that RP recruitment in double-mutant synapses is abnormally enhanced. Fig. 7 (D and E) also documents that RP recruitment in double-mutant larvae was rescued to control levels by the introduction of a copy of the *Scramb 1* gene.

We next evaluated the properties of synaptic transmission by recording nerve-evoked postsynaptic currents from larval NMJs (Acharya et al., 1998; Delgado et al., 2000; Kidokoro et al., 2004). Single-mutant synapses displayed transmitter release and plasticity properties that did not differ significantly from control (unpublished data). In contrast, synaptic transmission in the double mutant differed in several aspects from the control. We first observed that the frequency of spontaneous postsynaptic currents was significantly enhanced in the double mutant (Table III). We also found that release probability, quantal content, and nerve-evoked postsynaptic currents were significantly larger in the double mutant (Fig. 8, A and C; and Table III). On the other hand, the amplitude of current and the charge transferred by the release of a single quantum were, within experimental error, the same in control and double mutant (Table III). Fig. 8 A shows plots of nerve-evoked postsynaptic currents as a function of external Ca^{2+} concentration in double logarithmic fashion in control, double mutant, and P{*Scramb 1*}; double mutant. Data analysis revealed a similar Ca^{2+} cooperativity coefficient for nerve-evoked responses. However, in double-mutant synapses, the curve was shifted toward lower Ca^{2+} concentrations. We also recorded postsynaptic currents evoked by exposing synapses to a

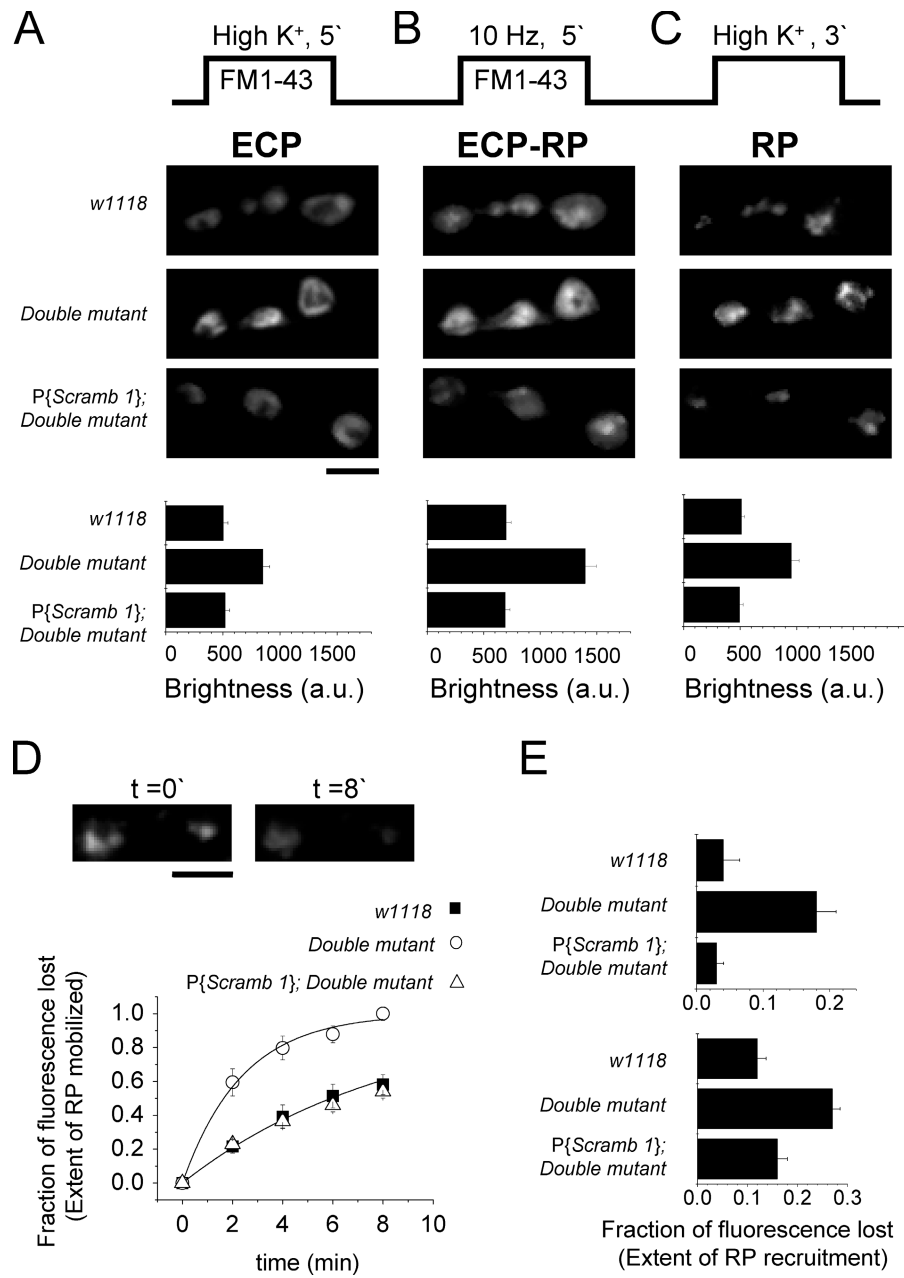


Figure 7. FM1-43 imaging. Studies of FM1-43 loading were made using the same FM1-43 stock, and the dye concentration was 5 μ M. Data shown in graphs was derived from 25 boutons from 10 different larvae \pm SEM. In all cases, fluorescence brightness was measured 3 min after extensive perfusion with a dye-free solution. (A) Studies of FM1-43 loading of ECP. Images are representative examples of dye-loading patterns in w1118, double mutant, and P{Scramb 1}; double mutant synaptic boutons. The graph below offers mean values of fluorescence brightness in w1118, double mutant, and P{Scramb 1}; double mutant synaptic boutons. (B) Studies of FM1-43 loading of SVs cycling through ECP and RP. Images are representative examples obtained in w1118, double mutant, and P{Scramb 1}; double mutant. Graph shows mean fluorescence brightness values \pm SEM in w1118, double mutant, and P{Scramb 1}; double mutant. (C) Studies of dye loading of SVs cycling through RP. Images are representative examples of dye-loading patterns of SVs cycling through RP, and the graph shows mean fluorescence brightness values \pm SEM. A *t* test revealed that in all cases differences in fluorescence brightness between double mutant, w1118, and P{Scramb 1}; double mutant are significant ($P < 0.05$). In all conditions, fluorescence brightness in control and P{Scramb 1}; double mutant was not statistically different. (D) Enhanced RP recruitment in double-mutant synapses and rescue in P{Scramb 1}; double mutant during high-frequency stimulation of the nerve. After dye loading of SVs cycling through RP was achieved using protocol explained in C, the time course of RP recruitment was evaluated by following the decline in fluorescence brightness during tetanic nerve stimulation at 10 Hz. The images above the graph show patterns of FM1-43 fluorescence at $t = 0$ and after 8 min of nerve stimulation at 10 Hz. Lines joining experimental points in graph are best fits to single exponential functions with time constants of 2.4 ± 0.2 min (double mutant) and 8.5 ± 0.2 min in control and P{Scramb 1}; double mutant. (E, top) Enhanced RP recruitment at rest, in the absence of high-frequency stimulation, in double mutant and rescue in P{Scramb 1}; double mutant. (bottom) Enhanced RP recruitment in double mutant during low-frequency stimulation (5 min) at 0.5 Hz in double mutant and rescue in P{Scramb 1}; double mutant. The extent of RP recruitment was evaluated 5 min after SVs cycling through the RP were loaded with FM1-43. Mean values of relative fluorescence brightness were derived from at least 10 different boutons from five different larvae. Bars, 5 μ m.

Table III. Comparison of characteristics of spontaneous response, quantal content, and evoked responses from *w1118* control and the double-mutant larval NMJs

Parameter	<i>w1118</i>	Double mutant	<i>P{Scramb 1}; Double mutant</i>
Quantal content (m)	0.35 ± 0.07 (9)	0.74 ± 0.14 (6)	0.32 ± 0.07 (5)
Release probability (pr)	0.29 ± 0.05 (9)	0.51 ± 0.06 (6)	0.27 ± 0.05 (5)
Frequency of spontaneous currents (Hz)	2.76 ± 0.51 (14)	5.61 ± 0.97 (20)	2.82 ± 0.44 (5)
Integral of current evoked by release of a single quanta (pC)	16.00 ± 0.41 (3)	16.46 ± 0.36 (3)	16.16 ± 0.28 (3)
Ca^{2+} cooperativity coefficient of nerve-evoked currents	3.40 ± 0.07 (5)	3.36 ± 0.12 (5)	3.47 ± 0.19 (4)
Amplitude of current evoked at 0.5 Hz (nA)	25.90 ± 3.66 (12)	41.64 ± 3.66 (11)	24.35 ± 3.93 (11)
Paired-pulse facilitation	1.41 ± 0.09 (27)	1.25 ± 0.14 (20)	1.45 ± 0.28 (8)
Tetanic facilitation	1.94 ± 0.19 (12)	1.68 ± 0.07 (12)	1.91 ± 0.23 (8)

Quantal content, probability of releasing at least one quanta, and frequency of spontaneous postsynaptic currents were monitored and estimated as described previously [Acharya et al., 1998] in a standard working solution containing $75 \mu\text{M}$, under conditions at which release probability is low. Also, quantal and charge transferred by release of a single quanta were studied as described previously [Acharya et al., 1998; Delgado et al., 2000]. Paired-pulse facilitation was defined as the ratio of the amplitude of the postsynaptic currents evoked by two consecutive stimulating episodes separated by 100 ms. Tetanic facilitation was taken as the ratio of amplitudes of last and first currents evoked by a 50-s tetanic stimulation at 10 Hz.

hyperosmotic 0.5 M sucrose solution (Acharya et al., 1998). As documented in Fig. 8 B, neurotransmitter release evoked by application of a 20-s hyperosmotic shock in the vicinity of the synapse was dramatically increased in the double mutant. Importantly, as documented in Fig. 8 and Table III, the synaptic defects in the double mutant were rescued by the introduction of a copy of the *Scramb 1* gene.

In further studies, we investigated plasticity properties of double-mutant synapses. Analysis of paired-pulse facilitation revealed that although the extent of facilitation of neurotrans-

mitter release in the double mutant was diminished relative to the control, this difference was not significantly different from the control (Table III). We next evaluated tetanic facilitation and posttetanic potentiation (PTP) by monitoring nerve-evoked currents using a stimulation protocol designed to monitor tetanic facilitation and PTP. Postsynaptic responses were evoked first by stimulating the nerve at 0.5 Hz for 20 s. This was followed by a period of tetanic stimulation at 10 Hz for 50 s. After the tetanic stimulation, the regimen was switched back to 0.5 Hz to monitor PTP. We found that the extent of facilitation of

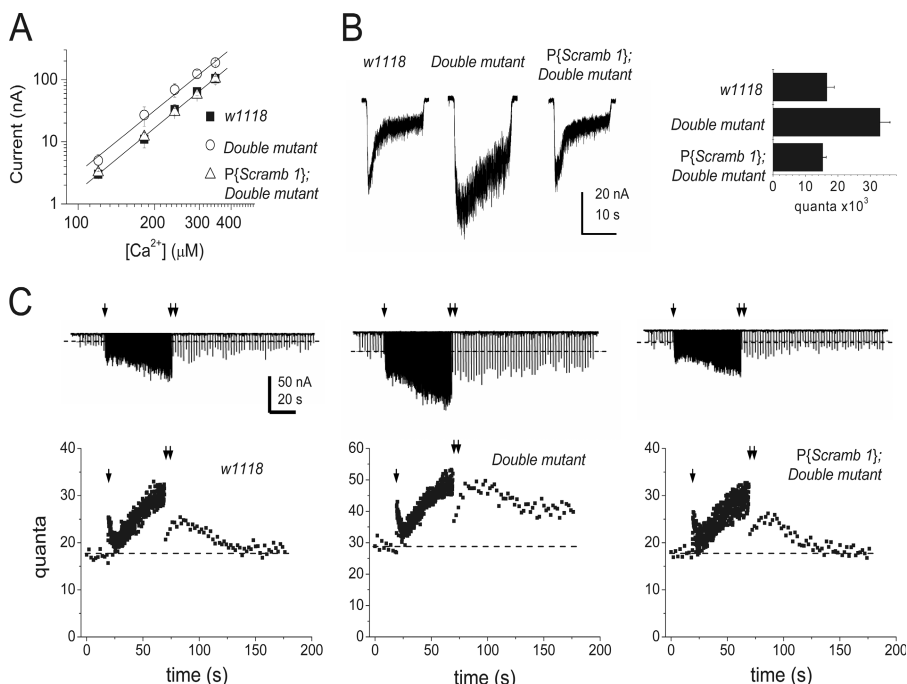


Figure 8. Abnormal properties of transmitter release in the double mutant and rescue in *P{Scramb 1}; double mutant* larval neuromuscular synapses. (A) Ca^{2+} dependence of transmitter release. Straight lines joining experimental points were built, with mean slope values derived from five different studies. (B) Studies of osmotic release of neurotransmitter. Records are representative examples of postsynaptic currents evoked by application of hyperosmotic solution, illustrating enlarged responses in double mutant and rescue in *P{Scramb 1}; double mutant*. The graph shows mean values of quantal content of currents evoked, estimated by dividing the integral of charge transferred during hyperosmotic shock divided by the integral of charge transferred by release of single quanta. Graph shows means of six different studies \pm SEM. Quantal content in double mutant was significantly above control and *P{Scramb 1}; double mutant* ($P < 0.05$). Within experimental error, quantal content of postsynaptic currents evoked by hyperosmotic shock was the same in control and *P{Scramb 1}; double mutant*. (C) Tetanic facilitation and PTP induced by high-frequency stimulation of the nerve at 10 Hz. The recordings document enlarged nerve-evoked responses in *P{Scramb 1}; double mutant* and are representative of post-

synaptic currents evoked during application of the protocol used to monitor tetanic facilitation and PTP. The graphs are mean quantal content of nerve-evoked currents during paradigm to monitor tetanic facilitation and PTP. Single arrows indicate the moment at which frequency of stimulation was switched from 0.5 to 10 Hz, leading to an increase in transmitter release (tetanic facilitation). Double arrows signal the moment at which stimulating frequency was switched back to 0.5 Hz. The discontinuous lines in the plots indicate quantal content of evoked currents before application of tetanic stimulation. Points in plot are means of at least seven different studies. Error bars were excluded for clarity.

transmitter release elicited by high-frequency stimulation of the nerve did not differ significantly from the control (Table III). On the other hand, we observed that PTP in the double mutant was abnormally prolonged. As shown in Fig. 8 C, in control synapse, nerve-evoked transmitter release decayed to values before stimulation (Fig. 8 C, bottom, discontinuous line) in ~50 s after the cessation of high-frequency stimulation. In contrast, in the double mutant, transmitter release remained significantly potentiated after 100 s, indicating altered short-term synaptic memory. Introduction of a genomic copy of the *Scramb 1* gene in the double mutant rescued PTP to normal. Also expression of a UAS–Scramb 2 gene driven by elav-GAL4 and neuronal promoter (elav-GAL4; UAS–Scramb 2; double mutant) rescued the content of ECP, RP, mobilization of RP pool of vesicles, postsynaptic current amplitude, quantal content, tetanic facilitation, and posttetanic facilitation to control levels (Fig. S5, available at <http://www.jcb.org/cgi/content/full/jcb.200506159/DC1>). In summary, our electrophysiological inquiries indicate that several aspects of synaptic function, including spontaneous, nerve-evoked release and PTP, are altered in the double mutant.

Despite changes in synaptic structure and physiology, overall synaptic function is not compromised in that the viability of the animal is not grossly affected in the double mutants. Thus, we believe that Scramblases have modulatory function in the secretory process of NMJs.

Discussion

Lipids are asymmetrically distributed between the two leaflets of the plasma membrane. Although the outer leaflet is enriched in choline phospholipids such as phosphatidylcholine and sphingomyelin, the inner leaflet contains anionic phospholipids such as PS and phosphatidylethanolamine. Although these lipids have a tendency to equilibrate along their concentration gradient, specific proteins that catalyze uni- or bidirectional transport of lipids from one leaflet to another maintain the asymmetry. One of the important players in this process is amorphophospholipid translocase. Although its molecular identity has not been definitely identified, a P-type ATPase (amorphophospholipid translocase) is thought to mediate this function (Wolfs et al., 2005). However, certain physiological and pathological conditions actively cause collapse of this asymmetry, resulting in scrambling of phospholipids. The most notable situation is in cells undergoing apoptosis wherein cell surface exposure of PS is one of the earliest detectable biochemical events. In fact, the annexin V binding assays for apoptotic cells is based on this exposure of PS. PS exposure has also been proposed as one of the signals that initiate the phagocytic process in cells targeted for phagocytosis. Lipid scrambling is thought to depend on one or more membrane proteins with lipid Scramblase activity. PLSCR1 was thus purified and identified as a putative Scramblase based on in vitro assays of transfer of lipids in bilayer. Subsequently, three other members of this family were discovered in humans and mice.

Mice lacking PLSCR1 and -3 have been generated. Phenotypic analysis of the mutants indicated that PLSCR1 mice showed a defective response of hematopoietic precursors

to granulocyte colony-stimulating and stem cell factors. PLSCR3 mice show insulin resistance, glucose intolerance, and dyslipidemia. Both knockout mice show no defects in lipid scrambling, suggesting that the presumed activity of this protein is not correct or that other members of the PLSCR family maintain the Scramblase activity. *D. melanogaster* has two definitely identified members of this family, and we have generated mutants in both proteins. Analyses of null (or severely hypomorphic) Scramblase mutants demonstrate that these proteins do not play a critical role in scrambling of phospholipids; instead, they have a modulatory role in the secretory process.

We have demonstrated that *D. melanogaster* Scramblases show an overlapping and ubiquitous expression throughout development, and they localize to the plasma membrane in all the tissues examined. The ubiquitous distribution suggests their participation in general housekeeping function involving plasma membrane. We used a Western blot-based genetic screen to obtain null mutants for each of the two Scramblases. We also recombined the two null mutants to generate double mutants of Scramblases. The viability and lack of any developmental defects in the single and double mutants and our studies with reaper expression in mutant animal backgrounds indicate that they do not play a deterministic role in scrambling of phospholipids. This notion is further supported by our data in S2 cells, where neither overexpression nor RNAi-mediated knock down of these proteins has any effect on the ability of resting or apoptotic cells to expose PS.

Our studies indicate that loss of both Scramblases results in alteration in both the organization and function of the larval NMJ. The synaptic phenotype of the double mutant includes an increase in the number of vesicles at the synapse (including docked vesicles), a fivefold increase in RP recruitment at rest, a twofold increase in release probability, and an abnormal PTP. The fact that the recruitment of vesicles from RP at rest in the absence of nerve stimulation is dramatically enhanced in the double mutants might explain in part the abnormally elevated number of docked vesicles seen in EM analysis. The increased cycling of vesicles through the RP, as indicated by the almost twofold increase in uptake of FM1-43 (Fig. 7 C), probably associates with the twofold increase in release probability and evoked release seen in the double-mutant synapse (Fig. 8, A and C; and Table III). Although increased resting Ca^{2+} levels can contribute to increased probability of release, we do not believe they are contributing to the double-mutant phenotype. For example, although RP recruitment at rest in the double mutant is enhanced fivefold relative to *w1118*, the probability of release is only twofold above normal. Because the cooperative factor of Ca^{2+} for transmitter release is approximately Ca^4 , an increase in Ca^{2+} at rest in the double mutant would be expected to have a much larger effect on release probability than on RP recruitment. On the other hand, an enhanced recruitment of SVs from RP could contribute to the increased number of SVs available for release observed in the double-mutant presynaptic terminals. An abnormal handling of Ca^{2+} might underlie the enhanced probability of release found in double-mutant synapses. Indeed, our results indicate a shift to left on the Ca^{2+} dependence of release, without a change in Ca^{2+} cooperativity, suggesting that

Ca^{2+} handling might be somehow abnormal in double-mutant synapses. However, paired-pulse facilitation is only slightly reduced in the double mutant synapse, arguing against a grossly abnormal handling of Ca^{2+} . Also, the rates of ECP exocytosis are known to depend significantly on Ca^{2+} (Kuromi and Kidokoro, 2003). However, contrary to what one would expect if Ca^{2+} levels were abnormally elevated, we observed that the rates of ECP exocytosis were the same in the control and double-mutant boutons. Thus, our observations would in principle rule out the possibility that grossly elevated Ca^{2+} levels underlie the abnormal synaptic phenotype observed in double-mutant synapses. In *D. melanogaster*, RP recruitment and transmitter release are fostered by elevations in cAMP levels at synaptic boutons, and RP recruitment is antagonized by PKA inhibitors (Kuromi and Kidokoro, 2000). Importantly, in a *dunce* mutant, with abnormally elevated cAMP levels, RP size is dramatically reduced, probably because of the excess translocation of SVs from RP (Kuromi and Kidokoro, 2000). We found that in spite of enhanced RP recruitment, RP size remains vigorous in the double mutant, as documented in Fig. 7 C. Thus, unlike *dunce*, enhanced RP recruitment in the double mutant is not accompanied by a reduced RP size. We cannot rule out the possibility that cAMP signaling is altered in double mutant synapses. If so, such alteration should allow for a significant enhancement in RP recruitment without a reduction in RP size. In short, our data seem to rule out in principle a grossly abnormal handling of Ca^{2+} or a severely altered operation of the cAMP cascade in double-mutant synapses. It is important to note that the effects of cAMP on transmitter release are not limited to fostering RP recruitment. There is evidence that cAMP-gated channels at the presynaptic terminal also play an important role, independent of PKA, in enhancing transmitter release in *D. melanogaster* (Cheung et al., 2006). In *D. melanogaster*, RP dynamics has also been associated to the actin cytoskeleton and to the actin binding myosin ATPase complex (Kidokoro et al., 2004; Verstreken et al., 2005). Further work should allow us to better understand the role of Scramblases in regulating RP dynamics and transmitter release in *D. melanogaster*. The fact that *D. melanogaster* Scramblases exhibit putative protein binding domains means it is possible that they are able to interact with other proteins and signaling pathways to participate in regulating transmitter secretion and SV trafficking at the presynaptic terminal. We provide the first evidence that Scramblases can play an important role in regulating RP recruitment, transmitter release, and short-term synaptic memory in *D. melanogaster*.

We believe that Scramblases have a general role in modulating regulated secretory process. In fact, earlier work done in mammalian Scramblases seems to support this notion, although this conclusion was not drawn in those studies. In one of the earlier studies, Scramblases were found to interact with thrombospondin 1, a secreted protein (Aho and Uitto, 1998). Interferon α , a secreted protein is a known up-regulator of Scramblase (Der et al., 1998; Zhou et al., 2000). Human Scramblase has been demonstrated to interact with human salivary leukocyte protease inhibitor, a secreted protein (Tseng and Tseng, 2000). Activation of Mast cells results in degranulation and secretion of a host of vasoactive amines, proteases, and proinflammatory

cytokines. Cultured mast cells RBL-2H3 activated with Fc ϵ RI resulted in up-regulation and phosphorylation of Scramblase protein (Pastorelli et al., 2001). Potentiation of the antiviral action of interferon by Scramblase has also been reported (Dong et al., 2004). PLSCR1 interacts with b-secretase (b-site amyloid precursor protein–cleaving enzyme), which is involved in secretion of the amyloid β -peptide (Kametaka et al., 2003). PLSCR1 mutants have no defect in scrambling but have deficient granulopoiesis, and PLSCR3 mutant mice display adiposity and dyslipidemia. Finally, B lymphocytes from a patient with Scott syndrome (whose red blood cells show defective scrambling), despite being deficient in Scramblase activity, have normal levels of PLSCR1, and the nucleotide sequence of the corresponding mRNA is identical to controls (Zhou et al., 1998). All the aforementioned results and our data from analyzing *scramb1*, *scramb2*, and the double mutants reveal a role for Scramblases in modulating regulated exocytosis and not in the scrambling of phospholipids.

Materials and methods

Identification and cloning of *D. melanogaster* Scramblases

A BLAST (basic local alignment search tool) search of the *D. melanogaster* genome database using the mammalian Scramb 2 sequence revealed the existence of two definitive members of Scramblase family of genes. The two Scramblases are Scramblase 67D (*Scramb 1*) and 63B (*Scramb 2*). *D. melanogaster* genome annotation project has listed these genes as CG1893 and CG32056. CG32056 (*Scramb 1*) is localized to the 67D region on the left arm of third chromosome, and CG1893 gene (*Scramb 2*) is localized to the 63B region on the left arm of third chromosome. A BLAST search against the cDNA database revealed the existence of several cDNA clones from the *D. melanogaster* collection maintained at the time by the Berkeley Drosophila Genome Project and Research Genetics. All clones whose 5' or 3' ends showed homology to the mouse Scramblases were obtained from Research Genetics and sequenced. Full-length cDNA clones corresponding to GM13876 for *Scramb 1* and GH10494 for *Scramb 2* genes were then used for all subsequent manipulations. The Scramblase cDNAs with appropriate cloning restriction sites were amplified, cloned, and sequenced. For transgenic overexpression in *D. melanogaster*, the appropriate cDNAs were cloned into pUAST vector, and for S2 cell overexpression they were cloned into pRMLHa-3 vector (a gift from L. Goldstein, University of California, San Diego, La Jolla, CA).

Fly stocks and husbandry

D. melanogaster stocks were cultured on standard maize meal agar and maintained at 25°C unless otherwise mentioned. The *Df(3L)AC1^{mroe-1}p⁰/TM3, Sb* *Df(3L)M21, kni[ri-1]p/Ln(3L)Rt33[L]f19, w⁻*; *P{w + mC = Actin}-Gal4* stocks were obtained from Bloomington Stock Center. Cyo, 2×GMR Rpr/Sco; MKRS/TM6B flies were obtained from K. White (Massachusetts General Hospital, Boston, MA).

Genetic screens and isolation of Scramblase mutants

w1118 males were aged for 3–4 d, starved overnight in empty vials, and subjected to chemical mutagenesis by feeding them on a diet of 25 μM EMS in 3% sucrose as previously described (Dolph et al., 1993; Acharya et al., 1998). These flies were then crossed en masse to virgin females with balanced third chromosomes. Single F1 males carrying a mutagenized chromosome over a third chromosome balancer were then crossed to virgin *Df(3L)AC1^{mroe-1}p⁰/TM3, Sb* flies in individual vials. The deficiency uncovers the 67D region. From each of these vials, a single progeny that carried the mutagenized chromosome over the deficiency was subjected to Western blot analysis for the loss of respective Scramblase antigen (Dolph et al., 1993; Acharya et al., 1998). Vials with lethal mutations in the interval uncovered by the deficiency were set aside to be used in transgenic rescue experiments, if necessary. Single fly heads were homogenized in SDS-PAGE buffer and loaded on gels. The separated proteins were transferred to nitrocellulose and incubated with affinity-purified rabbit polyclonal antibodies raised against the *Scramb 1* protein. A single null mutant was isolated in the screen.

To outcross all incidental and irrelevant mutations, the null mutant was backcrossed three times to *w1118* flies and selected by Western analysis. A similar approach was used to isolate the *scramb2* mutant. However, *Df(3L)M21, knifri-1p/ln(3L)Rt33[L]f19*, a deficiency that uncovers the 63B region, was used instead. Again, the null mutant was backcrossed three times to *w1118* controls to outcross all other mutations and selected by Western analysis.

Transgenic flies

The *Scramb 2* cDNA was amplified in frame with open reading frame of GFP gene and ligated to generate GFP–*Scramb 2* fusion. The gene was then cloned into pUAST vector and injected into embryos to generate transgenic flies expressing GFP–*Scramb 2* fusion. pUAST–*Scramb 2*-transgenic flies were generated. These lines were subsequently crossed to actin-Gal4 lines to drive its expression ubiquitously. A similar approach was attempted for *Scramb 1* gene, but no protein was detected in these flies either by Western analysis or by immunofluorescence. We presumed that the protein was misfolded and degraded. An 11.8-Kb *Sal*1–*Kpn*1 fragment of genomic DNA spanning the *Scramb 1* gene was cloned into pUAST, and transgenic lines were obtained. One of these mapped to the second chromosome and was used in the transgenic rescue experiments. The transgenic expression of *Scramb 1* protein was confirmed by Western analysis in the double-mutant background.

Antibodies

Rabbit polyclonal and monoclonal antibodies were raised against bacterially expressed, affinity-purified MBP–*Scramb 1* protein in which the *Scramb 1* protein was further cleaved off from MBP by factor Xa cleavage and purified by electro elution from polyacrylamide gels. Additionally, a COOH-terminal peptide antibody was raised against *Scramb 1*-derived peptide CFFEKAGNQETDRPGML and affinity purified. Rabbit polyclonal antibodies were raised against *Scramb 2* protein expressed using a pET3a expression system and purified by SDS-PAGE and electroelution. For Western analysis, affinity-purified anti-peptide *Scramb 1* antibody was used at 1:500 dilution and anti-*Scramb 2* antibody was used at 1:2,000–1:4,000. IPP antibodies were a gift from C. Zuker (University of San Diego, San Diego, CA). Anti-Fas II (1:500), anti-synaptotagmin (1:200), anti-cysteine string protein (1:25), anti-synataxin (1:200), and anti-DLG (1:200) monoclonal antibodies were obtained from Iowa Hybridoma Bank. Affinity-purified rabbit anti-synaptotagmin (1:1,000) antibody was a gift from M. Ramaswami and S. Sanyal (University of Arizona, Phoenix, AZ). Anti-HRP (1:500) and secondary antibodies (1:500) were obtained from Jackson ImmunoResearch Laboratories. Anti-CDase (1:3,000) antibodies have been described previously (Acharya et al., 2003, 2004; Rohrbough et al., 2004). The Notch antibody was a gift from M. Fortini (National Cancer Institute Frederick, Frederick, MD).

Immunofluorescence

Embryos and imaginal discs were collected and prepared for immunofluorescent staining as described previously (Patel, 1994). Tissues were incubated overnight with the antibodies (1:100–1:500 for anti-*Scramb 1* monoclonal and anti-*Scramb 2* rabbit polyclonal) at 4°C. These were costained with Alexa 568 or 488-conjugated goat anti-rabbit or goat anti-mouse IgG for 2 h at room temperature, washed, and mounted on Vectashield. For GFP visualization, the wing or eye imaginal discs were isolated from wandering third instar larvae, fixed in 4% formaldehyde, washed, and stained with propidium iodide for nuclear staining. For confocal microscopy, laser-scanning confocal microscopes (models 410 and 510; Carl Zeiss MicroImaging, Inc.) were used in most experiments, using a 63× oil objective, and pictures were obtained at resolutions ranging from 512 × 512 to 2048 × 2048. The pictures were pseudocolored in Photoshop (Adobe) for use in figures.

Electron microscopic examination

For electron microscopic examinations, wandering third instar larvae grown at 25°C were dissected and fixed using 2% glutaraldehyde and 4% formaldehyde in sodium cacodylate buffer. The tissues were postfixed in 1% osmium tetroxide and dehydrated in graded ethanol and propylene oxide. Specimens were embedded in epoxy resin (Embed-812) and thin sectioned. Transverse sections (90 nm) were stained with uranyl acetate and lead citrate and examined.

Genetic crosses

Mutant Scramblase flies (individual and double mutants) were crossed into GMR-Rpr background to evaluate the effects of these mutations in reaper-induced apoptosis. UAS–*Scramb 2* GFP flies were crossed to actin-Gal4 to drive expression ubiquitously.

Bacterial infections

Bacterial infection experiments were done as described previously (Rodriguez et al., 1996; Bernal and Kimrell, 2000). *Escherichia coli*, *Enterobacter cloacae* *B*₁₂, *Staphylococcus epidermidis*, and *Micrococcus reeseus* were gifts from D. Kimrell and R. Schoenfeld (University of California, Davis, Davis, CA). They were individually grown and pelleted. They were subsequently resuspended in LB collectively and pelleted again. The microorganism mixture was then injected into the thorax of individual flies using tungsten needles. A group of 10 individual flies were maintained in each vial, and the vials were replaced with a fresh vial every day. A total of 100 flies were infected for individual samples, and the experiment was repeated three times.

Scrambling index

Scramb 1 and *2* were cloned into pRMHA3 vector, and stable lines were established. The proteins were induced with 0.5 mM copper sulfate, and cells were harvested after 48 h of induction for Western analysis. A 900-bp fragment of *Scramb 1* and a 600-bp fragment of *Scramb 2* were PCR amplified with *E. coli* T7 polymerase site as described previously (Clemens et al., 2000; Worby et al., 2001) with minor modifications. RNA was synthesized using the T7 RNA polymerase kit (QIAGEN). The dsRNA were annealed by heating to 75°C for 20 min and slow cooling to room temperature. 1 µg of dsRNA was transfected to S2 cells in a 3-cm dish by Ca²⁺ phosphate transfection and media changed after 24 h. dsRNA-treated cells were evaluated for protein levels by Western analysis at 24, 48, and 72 h after transfection. For scrambling (apoptotic) index, stable cells induced for protein production for 48 h or cells treated with dsRNA for 48 h were treated with Actinomycin D. They were then incubated in annexin V binding buffer (10 mM Hepes, pH 7.4, 150 mM NaCl, and 2.5 mM CaCl₂) with annexin V-Alexa 488 propidium iodide. Stained cells were visualized using a confocal microscope (model 510). Approximately 300 cells were counted in three different fields for each experimental sample. Cells that were annexin V positive and propidium iodide negative were then used to calculate the percentage of cells that exposed PS on the surface (scrambling index).

Electrophysiology

Postsynaptic responses evoked by stimulation of the nerve were recorded from segments A2 or A3 of ventral longitudinal muscle 6 or 7 in third instar larvae using a two-electrode voltage clamp as reported previously in a standard working solution containing 128 mM NaCl, 2 mM KCl, 4 mM MgCl₂, 0.2 mM CaCl₂, 5 mM Hepes, and 36 mM sucrose, pH 7.3. Osmotic release of neurotransmitter was achieved by application of a hyperosmotic standard solution containing 500 mM sucrose and 50 µM CaCl₂ (Acharya et al., 1998; Delgado et al., 2000). The currents were recorded at –80 mV holding potential, and current amplitudes and integrals were analyzed using pClamp software (Axon Instruments, Inc.). Nerves were cut close to the ventral ganglia and sucked into the stimulating pipette. Evoked currents were elicited by stimulation of the nerve at the frequencies indicated using a programmable stimulator (Master-8; MPI). Data acquisition and analysis were done using pClamp software. The quantal content of nerve-evoked responses was estimated by dividing the current integral of individual nerve-evoked currents by the integral of the current evoked by the release of an individual quantum, as described previously (Acharya et al., 1998; Delgado et al., 2000).

Loading and unloading of FM1-43

Loading of ECP with FM1-43. Dye loading of vesicles cycling through ECP was achieved by exposing synaptic boutons for 5 min to high K⁺ external containing 10 µM FM1-43 (Invitrogen) as described by Kuromi and Kidokoro (2000).

Loading of RP with FM1-43. After dye loading of SVs cycling through ECP, nerve was stimulated at 10 Hz for 5 min in standard working solution containing FM1-43. FM1-43 was then removed by extensive rinsing with dye-free standard solution. Then, synaptic boutons were exposed for a second time to high K⁺ for 3 min to release SVs cycling through ECP, after which the external solution was extensively rinsed with standard working solution. The remaining FM1-43 fluorescence corresponds to SVs cycling through the RP (Delgado et al., 2000).

FM1-43 unloading. In all cases, FM1-43 unloading was monitored in a standard working solution at rest, in the absence of nerve stimulation or by stimulating the nerve at low (0.5 Hz) or high frequency (10 Hz) using a programmable stimulator.

Imaging

Synaptic boutons were imaged using an epi-fluorescence microscope (BX50WI; Olympus) with a 60× objective. Samples were excited for

200–300 ms via a controlled shutter system (Uniblitz; Vincent Associates). Images were captured with a 12-bit cooled charge-coupled device camera (SensiCam; PCO Imaging). Images were acquired and analyzed using Workbench 2.2 software (Axon Imaging). Results are from at least three synaptic boutons from a minimum of six different larvae per experimental condition. Fluorescence analysis was performed after correcting for bleaching and background.

Online supplemental material

Fig. S1 shows colabeling of Scramblase proteins with plasma membrane markers. Fig. S2 shows absence of Scramblase signals in synaptic boutons of the double-mutant larval NMJs. Fig. S3 shows staining of segmental nerves with Scramblases. Fig. S4 shows that Scramb 2 is present in pre and postmembranes of the larval NMJ. Fig. S5 shows rescue of the double-mutant synaptic phenotype by neuronal expression of Scramb 2. Online supplemental material is available at <http://www.jcb.org/cgi/content/full/jcb.200506159/DC1>.

We thank Drs. Charles Zuker, Kristin White, Vivian Budnik, Mark Fortini, Mani Ramaswami, Subhabrata Sanyal, and Deborah Kimbrell for flies, reagents and flies; Drs. Shyam Sharan, Mark Fortini, and Ira Daar for critical reading of the manuscript; and Jason de la Cruz for technical assistance.

This work was supported by funding from the intramural division of the National Cancer Institute. Work in the laboratory of P. Labarca is supported by FONDECYT and the Howard Hughes Medical Institute. Centro de Estudios Científicos is Millennium Institute funded in part by grants from Fundación Andes and the Tinker Foundation. P. Labarca is a Howard Hughes Medical Institute international scholar. R.A. Jorquerá was the recipient of a doctoral fellowship from Mejoramiento de la Calidad y la Equidad de la Educación Superior.

Submitted: 24 June 2005

Accepted: 8 March 2006

References

- Acharya, J.K., P. Labarca, R. Delgado, K. Jalink, and C.S. Zuker. 1998. Synaptic defects and compensatory regulation of inositol metabolism in inositol polyphosphate 1-phosphatase mutants. *Neuron*. 20:1219–1229.
- Acharya, U., S. Patel, E. Koundakjian, K. Nagashima, X. Han, and J.K. Acharya. 2003. Modulating sphingolipid biosynthetic pathway rescues photoreceptor degeneration. *Science*. 299:1740–1743.
- Acharya, U., M.B. Mowen, K. Nagashima, and J.K. Acharya. 2004. Ceramidase expression facilitates membrane turnover and endocytosis of rhodopsin in photoreceptors. *Proc. Natl. Acad. Sci. USA*. 101:1922–1926.
- Aho, S., and J. Uitto. 1998. Two-hybrid analysis reveals multiple direct interactions for thrombospondin 1. *Matrix Biol.* 17:401–412.
- Babcock, M., G.T. Macleod, J. Leither, and L. Pallanck. 2004. Genetic analysis of soluble N-ethylmaleimide-sensitive factor attachment protein function in *Drosophila* reveals positive and negative secretory roles. *J. Neurosci.* 24:3964–3973.
- Basse, F., J.G. Stout, P.J. Sims, and T. Wiedmer. 1996. Isolation of an erythrocyte membrane protein that mediates Ca^{2+} -dependent transbilayer movement of phospholipid. *J. Biol. Chem.* 271:17205–17210.
- Bernal, A., and D.A. Kimbrell. 2000. *Drosophila Thor* participates in host immune defense and connects translational regulator with innate immunity. *Proc. Natl. Acad. Sci. USA*. 97:6019–6024.
- Brand, A.H., and N. Perrimon. 1993. Targeted gene expression as a means of altering cell fates and generating dominant phenotypes. *Development*. 118:401–415.
- Brennan, C.A., and K.V. Anderson. 2004. *Drosophila*: the genetics of innate immune recognition and response. *Annu. Rev. Immunol.* 22:457–483.
- Bunch, T.A., Y. Grinblat, and L.S. Goldstein. 1988. Characterization and use of the *Drosophila* metallothionein promoter in cultured *Drosophila melanogaster* cells. *Nucleic Acids Res.* 16:1043–1061.
- Cheung, U., H.L. Atwood, and R.S. Zucker. 2006. Presynaptic effectors contributing to cAMP-induced synaptic potentiation in *Drosophila*. *J. Neurobiol.* 66:273–280.
- Clemens, J.C., C.A. Worby, N. Simonson-Leff, M. Muda, T. Maehama, B.A. Hemmings, and J.E. Dixon. 2000. Use of double-stranded RNA interference in *Drosophila* cell lines to dissect signal transduction pathways. *Proc. Natl. Acad. Sci. USA*. 97:6499–6503.
- Comfurius, P., P. Williamson, E.F. Smeets, R.A. Schlegel, E.M. Bevers, and R.F. Zwaal. 1996. Reconstitution of phospholipid scramblase activity from human blood platelets. *Biochemistry*. 35:7631–7634.
- Delgado, R., C. Maureira, C. Oliva, Y. Kidokoro, and P. Labarca. 2000. Size of vesicle pools, rates of mobilization, and recycling at neuromuscular synapses of a *Drosophila* mutant, *shibire*. *Neuron*. 28:941–953.
- Der, S.D., A. Zhou, B.R. Williams, and R.H. Silverman. 1998. Identification of genes differentially regulated by interferon alpha, beta, or gamma using oligonucleotide arrays. *Proc. Natl. Acad. Sci. USA*. 95:5623–5628.
- Dolph, P.J., R. Ranganathan, N.J. Colley, R.W. Hardy, M. Socolich, and C.S. Zuker. 1993. Arrestin function in inactivation of G protein-coupled receptor rhodopsin in vivo. *Science*. 260:1910–1916.
- Dong, B., Q. Zhou, J. Zhao, A. Zhou, R.N. Harty, S. Bose, A. Banerjee, R. Slee, J. Guenther, B.R. Williams, et al. 2004. Phospholipid scramblase 1 potentiates the antiviral activity of interferon. *J. Virol.* 78:8983–8993.
- Drysdale, R.A., M.A. Crosby, W. Gelbart, K. Campbell, D. Emmert, B. Matthews, S. Russo, A. Schroeder, F. Smutniak, P. Zhang, et al. 2005. FlyBase: genes and gene models. *Nucleic Acids Res.* 33:D390–D395.
- Ghezzi, A., Y.M. Al-Hasan, L.E. Larios, R.A. Bohm, and N.S. Atkinson. 2004. *slo* K^+ channel gene regulation mediates rapid drug tolerance. *Proc. Natl. Acad. Sci. USA*. 101:17276–17281.
- Hoffmann, J.A. 2003. The immune response of *Drosophila*. *Nature*. 426:33–38.
- Kametaka, S., M. Shibata, K. Moroe, S. Kanamori, Y. Ohsawa, S. Waguri, P.J. Sims, K. Emoto, M. Umeda, and Y. Uchiyama. 2003. Identification of phospholipid scramblase 1 as a novel interacting molecule with β -secretase (β -site amyloid precursor protein (APP) cleaving enzyme (BACE)). *J. Biol. Chem.* 278:15239–15245.
- Keshishian, H. 2002. Is synaptic homeostasis just wishful thinking? *Neuron*. 33:491–492.
- Keshishian, H., K. Broadie, A. Chiba, and M. Bate. 1996. The *Drosophila* neuromuscular junction: a model system for studying synaptic development and function. *Annu. Rev. Neurosci.* 19:545–575.
- Kidokoro, Y., H. Kuromi, R. Delgado, C. Maureira, C. Oliva, and P. Labarca. 2004. Synaptic vesicle pools and plasticity of synaptic transmission at the *Drosophila* synapse. *Brain Res. Brain Res. Rev.* 47:18–32.
- Kuromi, H., and Y. Kidokoro. 2000. Tetanic stimulation recruits vesicles from reserve pool via a cAMP-mediated process in *Drosophila* synapses. *Neuron*. 27:133–143.
- Kuromi, H., and Y. Kidokoro. 2003. Two synaptic vesicle pools, vesicle recruitment and replenishment of pools at the *Drosophila* neuromuscular junction. *J. Neurocytol.* 32:551–565.
- Kuromi, H., and Y. Kidokoro. 2005. Exocytosis and endocytosis of synaptic vesicles and functional roles of vesicle pools: lessons from the *Drosophila* neuromuscular junction. *Neuroscientist*. 11:138–147.
- Lavine, M.D., and M.R. Strand. 2002. Insect hemocytes and their role in immunity. *Insect Biochem. Mol. Biol.* 32:1295–1309.
- Leclerc, V., and J.M. Reichhart. 2004. The immune response of *Drosophila melanogaster*. *Immunol. Rev.* 198:59–71.
- Nordstrom, W., P. Chen, H. Steller, and J.M. Abrams. 1996. Activation of the reaper gene during ectopic cell killing in *Drosophila*. *Dev. Biol.* 180:213–226.
- Pastorelli, C., J. Veiga, N. Charles, E. Voignier, H. Moussu, R.C. Monteiro, and M. Benhamou. 2001. IgE receptor type I-dependent tyrosine phosphorylation of phospholipid scramblase. *J. Biol. Chem.* 276: 20407–20412.
- Patel, N.H. 1994. Imaging neuronal subsets and other cell types in whole-mount *Drosophila* embryos and larvae using antibody probes. In *Drosophila melanogaster: Practical Uses in Cell and Molecular Biology*. Vol. 44. L.S.B. Goldstein and E.A. Fyrberg, editors. Academic Press, San Diego. 445–487.
- Rodesch, C.K., and K. Broadie. 2000. Genetic studies in *Drosophila*: vesicle pools and cytoskeleton-based regulation of synaptic transmission. *Neuroreport*. 11:R45–R53.
- Rodriguez, A., Z. Zhou, M.L. Tang, S. Meller, J. Chen, H. Bellen, and D.A. Kimbrell. 1996. Identification of immune system and response genes, and novel mutations causing melanotic tumor formation in *Drosophila melanogaster*. *Genetics*. 143:929–940.
- Rohrbough, J., E. Rushton, L. Palanker, E. Woodruff, H.J. Matthies, U. Acharya, J.K. Acharya, and K. Broadie. 2004. Ceramidase regulates synaptic vesicle exocytosis and trafficking. *J. Neurosci.* 24:7789–7803.
- Schlegel, R.A., M.K. Callahan, and P. Williamson. 2000. The central role of phosphatidylserine in the phagocytosis of apoptotic thymocytes. *Ann. N. Y. Acad. Sci.* 926:217–225.
- Sims, P.J., and T. Wiedmer. 2001. Unraveling the mysteries of phospholipid scrambling. *Thromb. Haemost.* 86:266–275.
- Tepper, A.D., P. Ruurs, T. Wiedmer, P.J. Sims, J. Borst, and W.J. van Blitterswijk. 2000. Sphingomyelin hydrolysis to ceramide during the execution phase of apoptosis results from phospholipid scrambling and alters cell-surface morphology. *J. Cell Biol.* 150:155–164.

- Tseng, C.C., and C.P. Tseng. 2000. Identification of a novel secretory leukocyte protease inhibitor-binding protein involved in membrane phospholipid movement. *FEBS Lett.* 475:232–236.
- van den Eijnde, S.M., L. Boshart, E.H. Baehrecke, C.I. De Zeeuw, C.P. Reutelingsperger, and C. Vermeij-Keers. 1998. Cell surface exposure of phosphatidylserine during apoptosis is phylogenetically conserved. *Apoptosis*. 3:9–16.
- Verstreken, P., C.V. Ly, K.J. Venken, T.W. Koh, Y. Zhou, and H.J. Bellen. 2005. Synaptic mitochondria are critical for mobilization of reserve pool vesicles at *Drosophila* neuromuscular junctions. *Neuron*. 47:365–378.
- Wang, X.J., E.R. Reynolds, P. Deak, and L.M. Hall. 1997. The seizure locus encodes the *Drosophila* homolog of the HERG potassium channel. *J. Neurosci.* 17:882–890.
- White, K., M.E. Grether, J.M. Abrams, L. Young, K. Farrell, and H. Steller. 1994. Genetic control of programmed cell death in *Drosophila*. *Science*. 264:677–683.
- Wiedmer, T., J. Zhao, L. Li, Q. Zhou, A. Hevener, J.M. Olefsky, L.K. Curtiss, and P.J. Sims. 2004. Adiposity, dyslipidemia, and insulin resistance in mice with targeted deletion of phospholipid scramblase 3 (PLSCR3). *Proc. Natl. Acad. Sci. USA*. 101:13296–13301.
- Wolfs, J.L., P. Comfurius, J.T. Rasmussen, J.F. Keuren, T. Lindhout, R.F. Zwaal, and E.M. Bevers. 2005. Activated scramblase and inhibited aminophospholipid translocase cause phosphatidylserine exposure in a distinct platelet fraction. *Cell. Mol. Life Sci.* 62:1514–1525.
- Worby, C.A., N. Simonson-Leff, and J.E. Dixon. 2001. RNA interference of gene expression (RNAi) in cultured *Drosophila* cells. *Sci. STKE*. 2001:PL1.
- Zhou, Q., J. Zhao, J.G. Stout, R.A. Luhm, T. Wiedmer, and P.J. Sims. 1997. Molecular cloning of human plasma membrane phospholipid scramblase. A protein mediating transbilayer movement of plasma membrane phospholipids. *J. Biol. Chem.* 272:18240–18244.
- Zhou, Q., P.J. Sims, and T. Wiedmer. 1998. Expression of proteins controlling transbilayer movement of plasma membrane phospholipids in the B lymphocytes from a patient with Scott syndrome. *Blood*. 92:1707–1712.
- Zhou, Q., J. Zhao, F. Al-Zoghaibi, A. Zhou, T. Wiedmer, R.H. Silverman, and P.J. Sims. 2000. Transcriptional control of the human plasma membrane phospholipid scramblase 1 gene is mediated by interferon- α . *Blood*. 95:2593–2599.
- Zhou, Q., J. Zhao, T. Wiedmer, and P.J. Sims. 2002. Normal hemostasis but defective hematopoietic response to growth factors in mice deficient in phospholipid scramblase 1. *Blood*. 99:4030–4038.
- Zimmermann, K.C., J.E. Ricci, N.M. Droin, and D.R. Green. 2002. The role of ARK in stress-induced apoptosis in *Drosophila* cells. *J. Cell Biol.* 156:1077–1087.
- Zwaal, R.F., P. Comfurius, and E.M. Bevers. 2005. Surface exposure of phosphatidylserine in pathological cells. *Cell. Mol. Life Sci.* 62:971–988.